

High-Field Galvanomagnetic Properties of Indium†

JAMES C. GARLAND AND R. BOWERS

Laboratory of Atomic and Solid State Physics, Cornell University, Ithaca, New York 14850

(Received 12 August 1969)

Measurements are reported of the high-field magnetoresistance and Hall effect of both single-crystal and polycrystalline indium. Although the magnetoresistance exhibited no pronounced crystal anisotropy, substantial deviations from Kohler's rule were observed. It is found that both the longitudinal and transverse magnetoresistance increase linearly in high-purity specimens but not in impure material. Other deviations from Kohler's rule are attributed to small-angle electron-phonon scattering. The Hall coefficient of indium was found to decrease slightly with increasing magnetic field. Measurements were made using dc techniques as well as the standing-wave helicon method; in addition, solutions of the helicon wave equation for a finite cylinder transverse to the magnetic field are considered.

I. INTRODUCTION

IN this paper, we report on the results of a general survey of the high-field galvanomagnetic properties of indium. Specifically, we have measured the magnetoresistance and Hall coefficient of indium in both single-crystal and polycrystalline specimens. Using anisotropy measurements about principal crystal directions, we have attempted to detect the presence of open orbits, predicted by recent Fermi-surface calculations,¹ as well as to investigate the possibility of magnetic breakdown occurring at moderate-field strengths. In polycrystalline specimens of indium we have investigated the validity of Kohler's rule in the high-field limit. Hall-coefficient measurements in this field range were also made and slight discrepancies were found between our observations and the traditional theory of the Hall effect.

The results of previous studies in indium single crystals have generally agreed that the magnetoresistance exhibits only a moderate amount of anisotropy, with none of the sharp resistance maxima that are typical of metals with open Fermi surfaces. The transverse magnetoresistance of randomly oriented single crystals of indium was studied by Borovik and Volotskaya² and later by Volotskaya³ in fields up to 35 kG. The rotation diagrams for their samples show a small orientation dependence of the magnetoresistance with a maximum deviation from isotropy of 15%. However, there is no obvious crystal symmetry in their data, so it is not clear whether the observed anisotropy is actually due to the indium crystal structure or whether it is merely a consequence of sample probe effects.⁴ Recently, Gaidukov⁵ has studied the

transverse magnetoresistance in high-purity oriented single crystals of indium whose major axes were aligned along the [001], [110], and [101] crystal directions. His measurements, which were performed at field strengths below 24 kG, show a small deviation from isotropy of not more than 7%. Our own measurements of the transverse magnetoresistance in single-crystal indium samples were performed at somewhat higher fields than previously reported. Although there is evident crystalline symmetry in rotation diagrams obtained about principal crystal axes, our measurements are nonetheless in agreement with previous results which show little pronounced anisotropy.

In addition to measurements on single-crystal specimens, we have also investigated the magnetoresistance of polycrystalline indium. Our intent was to study two basic features of the magnetoresistance: (a) the extent to which saturation occurs at high-field values, and (b) the validity of Kohler's rule in the high-field limit. Measurements of the magnetoresistance of polycrystalline indium have been reported by several authors generally in connection with size-effect studies. Observations by Olsen⁶ below 10 kG show saturation of both the transverse and longitudinal magnetoresistance to occur in bulk samples of indium. Measurements by other authors^{7,8} generally confirm this finding, although for some specimens the saturation is not yet complete at the highest field employed. Observations by Blatt, Burmester, and LaRoy⁹ of the transverse magnetoresistance of polycrystalline indium wires, however, suggest that the magnetoresistance increases linearly with field in the high-field limit. This non-saturation, which was also observed by Gaidukov⁵ in some single-crystal specimens, is in direct contrast to the theory of magnetoresistance proposed by Lifshitz,

† Work supported by the U. S. Atomic Energy Commission, under Contract No. AT(30-1)-2150, Technical Report No. NYO-2150-55 and by the Advanced Research Projects Agency, through the Materials Science Center at Cornell University, MSC Report No. 1195.

¹ N. W. Ashcroft and W. E. Lawrence, *Phys. Rev.* **175**, 938 (1968).

² E. S. Borovik and V. G. Volotskaya, *Zh. Eksperim. i Teor. Fiz.* **38**, 261 (1968) [English transl.: *Soviet Phys.—JETP* **11**, 189 (1960)].

³ V. G. Volotskaya, *Zh. Eksperim. i Teor. Fiz.* **45**, 49 (1963) [English transl.: *Soviet Phys.—JETP* **18**, 36 (1964)].

⁴ N. E. Alekseevskii, N. B. Brandt, and T. I. Kostina, *Zh.*

Eksperim. i Teor. Fiz. **34**, 1339 (1958) [English transl.: *Soviet Phys.—JETP* **7**, 924 (1958)].

⁵ Yu. P. Gaidukov, *Zh. Eksperim. i Teor. Fiz.* **49**, 1049 (1965) [English transl.: *Soviet Phys.—JETP* **22**, 730 (1966)].

⁶ J. L. Olsen, *Helv. Phys. Acta* **31**, 713 (1958).

⁷ P. Wyder, *Physik Kondensierten Materie* **3**, 263 (1965).

⁸ F. de la Cruz, M. E. de la Cruz, and J. M. Cotignola, *Phys. Rev.* **163**, 575 (1967).

⁹ F. J. Blatt, A. Burmester, and B. LaRoy, *Phys. Rev.* **155**, 611 (1967).

Azbel, and Kaganov,¹⁰ which predicts that strict saturation should always occur for uncompensated metals with closed Fermi surfaces. However, a linear term is known to occur in the high-field magnetoresistance of many simple metals, including potassium,^{11,12} sodium,¹³ and aluminum,¹⁴ and is thought to result from details of the scattering process which cannot be incorporated into a simple relaxation-time approximation. We have observed a linear term in both the transverse and longitudinal magnetoresistance of many indium samples and have determined some of the parameters on which it depends.

There is general agreement in the literature that Kohler's rule is extremely well obeyed in indium for $\omega_c\tau < 1$. However, in the high-field regime, deviations from Kohler's rule have been observed in indium by several authors. Measurements by Olsen⁶ show a slight temperature enhancement of the Kohler variable $\Delta\rho/\rho(0)$ in bulk specimens at high fields. Because this enhancement, which has been reported by several authors,^{7,9} is most pronounced in thin specimens, it has generally been attributed to the size-effect mechanism. Our observations suggest that it may also be important in bulk material.

In addition to the magnetoresistance, we have also measured the high-field Hall coefficient of both polycrystalline and single-crystal indium in fields up to 140 kG. Previous measurements of the Hall coefficient of indium¹⁵⁻¹⁷ have been in agreement that the coefficient is satisfactorily explained in terms of the traditional theory which maintains that, for $\omega_c \gg 1$, $R(H) \rightarrow 1/ec(n_1 - n_2)$; here n_1 and n_2 represent the carrier density of the hole and electron bands, respectively. Our measurements show, on the other hand, that there is a slight variation of the indium Hall coefficient in this field region, with R decreasing slightly at the higher fields. Penz has previously reported such a field decrease in the Hall coefficient of potassium using the helicon wave technique.^{12,18,19} Our measurements were performed using both the dc and helicon method, and we have observed a decrease of $R(H)$ in a number of metals besides indium.²⁰

II. EXPERIMENTAL DETAILS

A. Helicon Method

In these experiments both the dc and the helicon methods were used to measure the Hall coefficient and magnetoresistance. The helicon technique offers the advantages inherent in a probeless method; this was particularly important in anisotropy studies in single-crystal samples where dc probe effects are known to have complicated much of the existing data.^{4,5} Furthermore, with the helicon method it is not necessary to reverse the direction of the magnetic field for each measurement; this is a significant advantage when superconducting solenoids with lengthy ramp times are used.

The helicon method is not without its own disadvantages, however. While helicon measurements of the Hall coefficient in single crystals are relatively unambiguous, magnetoresistance measurements are complicated by the fact that the helicon samples the average tensor element $(\rho_{xx} + \rho_{yy})$ over the entire Fermi surface.²¹ This is not important when H is oriented along a fourfold symmetry direction, but it makes interpretation of the data rather confusing when this symmetry does not exist. Furthermore, one must exercise considerable care to ensure that the sample being investigated is firmly cemented to the sample holder; if this is not done, sample vibration can occur with the effect of degrading the helicon amplitude. In rotation experiments this can be particularly troublesome at fields above 20 kG and leads to rotation diagrams not unlike those caused by probe effects in dc magnetoresistance studies.

Figure 1(a) shows the instrumentation used in the conventional standing-wave helicon experiments. An audiofrequency voltage is generated in the audio-oscillator, converted to an ac current by a power amplifier, and connected to a helmholtz coil which supplies the driving field for the helicon. The signal voltage from the pickup coil is then amplified by a broad-band ac amplifier, and after integration is applied to the X - Y recorder. Simultaneously, a voltage proportional to the frequency of the driving signal is applied to the X input of the recorder. The resulting trace corresponds to the modulus of the standing-wave resonance. Because the signal voltages were typically of the order of mV at the high fields used in this experiment, more sophisticated synchronous detection techniques were not required.

In this experiment, two sample geometries were used: Cylindrical samples were used for single-crystal anisotropy measurements, while for helicon measurements in polycrystalline indium, rectangular flat-plate samples were used. Solutions of the helicon boundary-value problem for the rectangular-plate geometry are well known; in the high-field limit the relevant expressions

¹⁰ I. M. Lifshitz, M. Ya. Azbel, and M. I. Kaganov, *Zh. Eksperim. i Teor. Fiz.* **31**, 63 (1956) [English transl.: *Soviet Phys.—JETP* **4**, 41 (1957)].

¹¹ P. A. Penz and R. Bowers, *Solid State Commun.* **5**, 341 (1967).

¹² P. A. Penz and R. Bowers, *Phys. Rev.* **172**, 991 (1968).

¹³ F. E. Rose, Ph.D. dissertation, Cornell University, 1964 (unpublished).

¹⁴ R. J. Balcombe, *Proc. Roy. Soc. (London)* **A275**, 113 (1963).

¹⁵ R. G. Chambers and B. K. Jones, *Proc. Roy. Soc. (London)* **A270**, 417 (1962).

¹⁶ T. Amundsen, *Proc. Phys. Soc. (London)* **88**, 757 (1966).

¹⁷ J. N. Cooper, P. Cotti, and F. B. Rasmussen, *Phys. Letters* **19**, 560 (1965).

¹⁸ P. A. Penz, Ph.D. dissertation, Cornell University, 1966 (unpublished).

¹⁹ P. A. Penz, *Phys. Rev. Letters* **20**, 725 (1968).

²⁰ J. C. Garland (unpublished).

²¹ P. A. Penz, *J. Appl. Phys.* **38**, 4047 (1967).

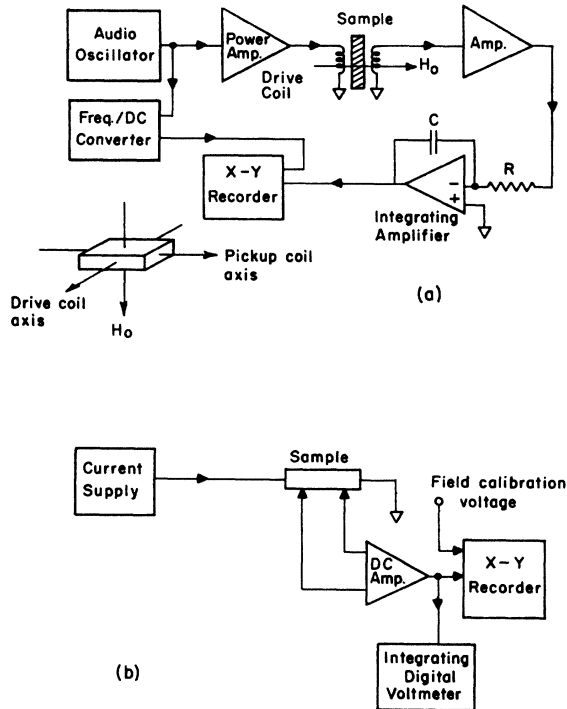


FIG. 1. Block diagrams of instrumentation used (a) in standing-wave helicon experiments; (b) used in dc experiments.

for the fundamental standing-wave resonance are given by¹⁵

$$\omega_r = \alpha R H_0 (1 + 1/u^2)^{1/2}, \quad (1a)$$

$$V_p \propto u. \quad (1b)$$

Here ω_r corresponds to the fundamental helicon resonant frequency, and V_p represents the integrated signal voltage. The quantity $u = RH_0/\rho(H_0)$ is the tangent of the Hall angle and is related to the Q of the resonance by $u = (4Q^2 - 1)^{1/2}$. Thus, by measuring Q , ω_r , and V_p the Hall coefficient R and transverse magnetoresistance $\rho(H_0)$ can be obtained. The coefficient α is a constant which is characteristic of the particular geometry of the sample.

The boundary-value problem for a standing-wave resonance in a cylinder whose major axis is transverse to the static magnetic field has never been solved. We consider this problem in the Appendix and show that Eqs. (1a) and (1b) are still applicable for this situation provided that the coefficient α is suitably changed to account for the different geometry. Although the solutions we have obtained for the transverse cylinder problem are only approximately correct, the actual numerical value of α is immaterial to the present experiment since we are concerned only with relative variations of R and $\rho(H_0)$.

B. dc Method

Figure 1(b) shows the instrumentation used for our conventional 4-probe dc measurements of the magneto-

resistance and Hall coefficient. The sample current was supplied by a constant-current source with a stability of better than 0.05%. The dc voltage from the potential probes was amplified by a low-noise amplifier and displayed by the digital integrating voltmeter; with integration times of about 1 sec this system could resolve voltage changes of about 1 n.v. Simultaneous field plots of the probe voltage could also be traced on the X-Y recorder. Both superconducting magnets and water-cooled copper solenoids were used; field measurements are believed accurate to better than 0.1% and are traceable to NMR calibration.

A variety of potential probe material was used including indium, copper, and phosphor bronze, and probes were both soldered and cold welded to the specimens. Considerable care was spent in minimizing thermoelectric offset voltages; soft-drawn copper was used for all wiring while terminal blocks were heat sunk to large blocks of copper. For Hall-effect measurements two samples were wired in series and Hall-voltage measurements were performed simultaneously on each sample. All dc measurements are taken to be the average of normal and reverse field directions.

C. Sample Preparation

The indium starting material used in this experiment was obtained from the American Smelting and Refining Company and from Cominco, Inc. Polycrystalline flat plates were prepared by pressing blocks of indium between stainless-steel plates with Mylar sheets separating the indium from the stainless steel. Polycrystalline cylinders of indium were extruded from stainless-steel dies.

Single-crystal indium cylinders were obtained by a crystal-pulling technique; an oriented seed crystal was lowered into a molten pool of indium and then slowly withdrawn. By carefully controlling the temperature of the melt and the pulling speed, cylinders with diameter variations of no more than a few percent could be obtained; the crystallographic orientation of each cylinder was then verified by x-ray analysis. Before a run each sample was annealed at 50°C in air for several hours and then loaded into the sample holder. After each run the sample was x rayed again to verify that no significant strain was introduced by confinement in the sample holder.

III. EXPERIMENTAL RESULTS

A. Magnetoresistance and Hall Effect in Single-Crystal Indium (Helicon Method)

In Fig. 2 are shown magnetoresistance rotation diagrams for three single-crystal indium specimens. In Fig. 2(a) the transverse magnetoresistance is given for an unoriented single crystal whose cylindrical axis was tilted about 10° from the [110] crystalline axis. The anisotropy evident in this specimen was greater than

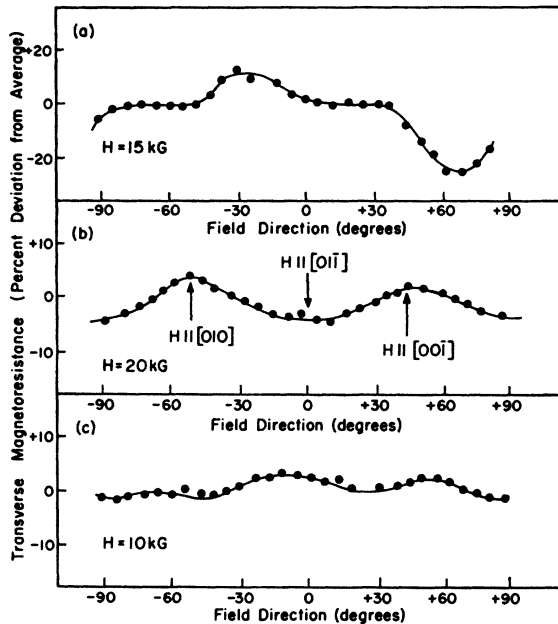


FIG. 2. Rotation diagram of transverse magnetoresistance of three single-crystal indium specimens; (a) Unoriented crystal; (b) rotation about $[100]$ axis; (c) rotation about $[111]$ axis.

that observed in any other sample and corresponds to about a 15% deviation from the average value.

In order to determine whether sample nonuniformity could be responsible for the apparent magnetoresistance anisotropy, we performed measurements on an intentionally deformed polycrystalline sample. In this highly deformed specimen, whose cross section was roughly elliptical with axes in the ratio 2:1, the measured anisotropy of both the helicon amplitude and frequency was less than 3%. Therefore, it appears that dimensional uniformity is not a particularly stringent criterion for performing accurate helicon measurements of the magnetoresistance and Hall coefficient.

Figure 2(b) shows the magnetoresistance rotation diagram for a specimen whose cylindrical axis was oriented to within 1° of the $[100]$ crystalline axis. The maximum deviation from isotropy about this axis was only about 5%, with the magnetoresistance exhibiting maximum values for the field aligned along the $[010]$ and $[001]$ directions. Although indium has a tetragonal structure, the c/a ratio is less than 1.1, so that the rotation diagram shows nearly cubic symmetry. There is a marked resemblance between Fig. 2(b) and data obtained by Balcombe¹⁴ for a similarly oriented aluminum crystal; the magnetoresistance maxima and minima have the same broad shape and occur in the same crystal directions in the two materials. The Hall coefficient for this specimen was invariant to within the experimental accuracy of 1%.

In Fig. 2(c) is shown the magnetoresistance rotation diagram for an indium crystal whose cylindrical axis was oriented to within 1° of the $[111]$ axis. Al-

though the change in magnetoresistance was found to deviate less than 3% from the average value, as expected from the symmetry of the crystal, there appear to be three broad maxima in the rotation diagram occurring about 60° apart. The Hall coefficient of this specimen was isotropic to within the experimental error.

In general, no sharp maxima or minima were found in either the magnetoresistance or Hall coefficient of any of our samples. Furthermore, we found no difference in the field dependence of the magnetoresistance for a given specimen in different crystal directions; that is, the shape of the rotation diagrams remained field-independent up to 58 kG, which was the highest field used. We performed particularly careful measurements in principal crystalline directions, but could detect no qualitative difference between the magnetoresistance of our single-crystal samples and the polycrystalline samples discussed in Sec. III B. Although in high-purity samples the magnetoresistance increased linearly with field, we could find no evidence for a quadratic field dependence.

Thus, we are unable to detect the presence of open carrier orbits as predicted by recent indium band-structure calculations.¹ However, these orbits, which should occur in the $[100]$ and $[010]$ directions, are expected to be very small in number and possibly are not observable in fields below 60 kG.

B. Transverse and Longitudinal Magnetoresistance in Polycrystalline Indium (dc Method)

In Fig. 3 is shown the field dependence of the transverse magnetoresistance of three polycrystalline indium specimens of different purities. For curve C, which is representative of specimens whose residual resistance ratio $\rho(290)/\rho(4.2)$ is under 8000, the magnetoresistance has a broad "knee" which occurs at $\omega_c\tau \approx 5-10$. At

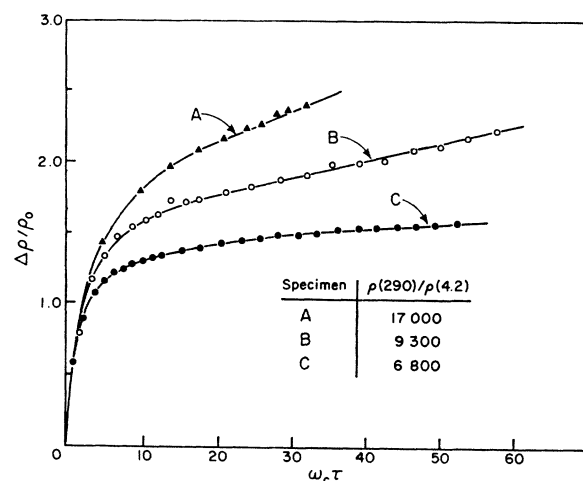


FIG. 3. Transverse magnetoresistance of three polycrystalline indium specimens showing deviations from Kohler's rule.

higher values of $\omega_c\tau$ the magnetoresistance does not saturate but increases approximately as $H^{1/2}$, so that in the high-field limit the magnetoresistance is described fairly well by the relation $\Delta\rho/\rho_0 \approx a + b(\omega_c\tau)^{1/2}$, where a is a constant term approximately equal to 1.25 and b is a constant equal to 0.04. At higher sample purities, represented by curves A and B in Fig. 3, the "knee" in the transverse magnetoresistance becomes broader, persisting to higher values of $\omega_c\tau$. In addition, the field dependence of the magnetoresistance becomes more pronounced in the high-field limit with $\Delta\rho/\rho_0$ increasing linearly with magnetic field. As is evident from Fig. 3, these impurity-induced deviations from Kohler's rule can be quite large with sample-to-sample variations in $\Delta\rho/\rho_0$ differing by a factor of 3 or more at moderate fields.

Although the linear term in the magnetoresistance is definitely most evident in high-purity specimens, our observations suggest that there may not be a simple correlation between sample impurity content and the slope of the linear term. Rather, it appears that in very pure samples the details of the sample history such as the preparation technique, annealing time, and sample holding method all appear to influence the slope. Generally, the greater the degree of stress exerted on the sample before making measurements, the greater is the observed linear magnetoresistance. In samples of only moderate purity, the influence of these effects is correspondingly smaller, becoming nonexistent in specimens with great impurity content.

Figure 4 shows the longitudinal magnetoresistance of three polycrystalline indium samples of different purities. In contrast to the transverse magnetoresistance, the longitudinal magnetoresistance of our lowest-purity sample, curve C in Fig. 4, shows strict saturation in the high-field limit with $\Delta\rho/\rho_0 = 0.6$. In addition, the knee of the magnetoresistance curve, which occur; at $\omega_c\tau \approx 2\pi$, is somewhat sharper than the cor-

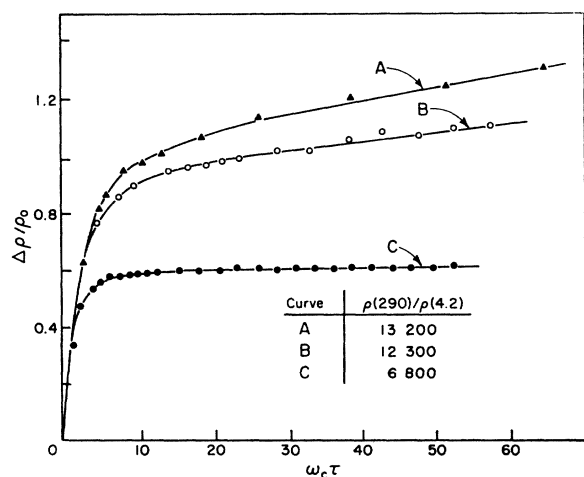


Fig. 4. Longitudinal magnetoresistance of three polycrystalline indium specimens showing deviations from Kohler's rule.

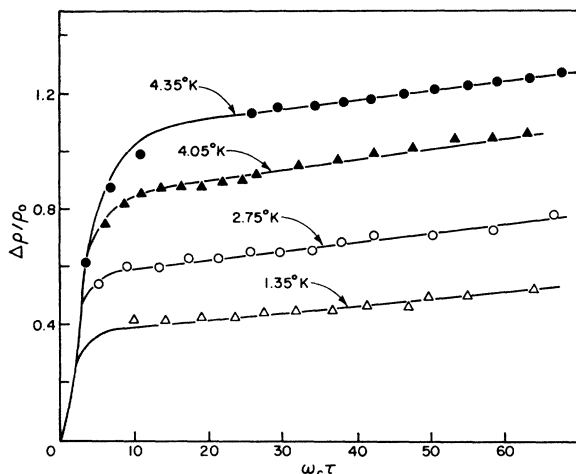


Fig. 5. Longitudinal magnetoresistance of polycrystalline indium specimen at different temperatures showing deviations from Kohler's rule.

responding knee in the transverse magnetoresistance. Thus, at moderate- or low-purity levels, the longitudinal magnetoresistance is in excellent agreement with the theory of Lifshitz, Azbel, and Kaganov.¹⁰ However, in higher-purity samples the knee becomes broader, and significant deviations from Kohler's rule become apparent with the magnetoresistance exhibiting the characteristic linear field dependence observed in the transverse measurements. For high-purity specimens the longitudinal magnetoresistance in the high-field limit can be represented to a good approximation by the relationship $\Delta\rho/\rho_0 = a + b(\omega_c\tau)$, where a and b are constants whose measured value tends to increase with diminishing sample impurity content. However, the previous comments about the influence of sample history apply to this situation also, so that we can report no simple observed relationship between the coefficients a and b and impurity content.

In addition to deviations from Kohler's rule in samples of differing impurity content, we have also observed a temperature-induced enhancement of the magnetoresistance. This mechanism affects both the transverse and longitudinal magnetoresistance in the same way, so that the ratio of the transverse to longitudinal magnetoresistance $\Delta\rho(\text{trans})/\Delta\rho(\text{long})$ for any given sample remains independent of temperature (the specific ratio may vary somewhat from sample to sample, however). Figure 5 shows the longitudinal magnetoresistance of a polycrystalline indium specimen at four different temperatures. The residual resistance ratio $\rho(290)/\rho(0)$ of this sample was about 23 000, and a threefold increase in $\Delta\rho/\rho_0$ occurred as the temperature was increased 1.35–4.35°K.

It is worth remarking on the differences between the effects of thermal scattering and impurity scattering on the magnetoresistance. As is evident from Fig. 5, thermal scattering enhances the magnetoresistance,

while the opposite occurs with increases in impurity scattering. Furthermore, the effects of increasing the temperature is merely to add a constant term to the high-field magnetoresistance, but not to change the field dependence of $\Delta\rho/\rho_0$; an increase in impurity resistance, on the other hand, tends to suppress the field dependence. This temperature enhancement of the magnetoresistance does not occur at a uniform rate: Some specimens show a much stronger temperature enhancement than other samples, yet there does not appear to be any simple correlation with sample impurity content. The pathology of this situation is illustrated in Fig. 6, where we have plotted the longitudinal magnetoresistance at fixed $\omega_c\tau$ as a function of lattice resistivity for three samples. All of these measurements were made at temperatures below 4.5°K, and it can be seen that in this temperature range $\Delta\rho/\rho_0$ increases linearly with lattice resistivity. However, it is also apparent that there is no clear systematic variation of either the $T=0$ value of $\Delta\rho_0/\rho$ or the degree of thermal enhancement with impurity content. In a statistical sense, however, our observations suggest that the thermal enhancement is greatest in high-purity specimens.

In summary, therefore, it appears that in indium both the longitudinal and transverse magnetoresistance depend on the high-field limit on the mutual interactions of impurity scattering and thermal scattering as well as on crystal imperfections such as lattice defects and strain. The effect of impurity scattering is to reduce or depress the effects of the other mechanisms; in view of this fact it is our belief that the magnetoresistance of an "ideal" crystal at $T=0$ is probably nearly the same as that measured in our impure speci-

mens represented by curves C in Figs. 4 and 5. At low temperatures, electron-phonon scattering enhances the saturation value of the magnetoresistance but does not affect its field dependence. While we have not studied systematically the influences of strain, defects, slip planes, etc., it does appear that some or all of these mechanisms can enhance the magnetoresistance of indium as well as introduce a linear field dependence at large values of $\omega_c\tau$.

C. High-Field Hall Coefficient of Polycrystalline Indium (Helicon and dc Method)

We have measured the field dependence of the Hall coefficient in a number of polycrystalline indium samples in fields 20–140 kG. In all of these samples we have observed the Hall coefficient to decrease slightly with increasing field, usually about 2% over the field range investigated. Although this field dependence does not appear to be a bulk property of indium we cannot yet report any obvious correlation with sample size, impurity content, or preparation history. The smallest relative decrease observed was 0.5%.

In Fig. 7 is shown the field dependence of the Hall coefficient for two representative specimens. The data in Fig. 7(a) were obtained from conventional dc measurements, while those in Fig. 7(b) were obtained using the helicon wave technique. In Fig. 7(a), the Hall coefficient is seen to decrease approximately 3.5% as the field was increased 20–100 kG this was the greatest change observed for any of our samples. In Fig. 7(b) a more typical decrease of 2% was observed over the same field range for the Hall coefficient of a different specimen.

There is at present no known explanation for this effect, although Penz^{12,19} has reported a similar behavior in the Hall coefficient of potassium from helicon mea-

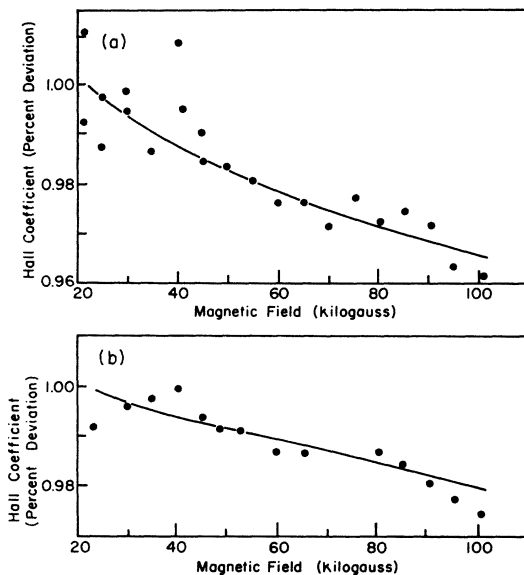


FIG. 6. Enhancement of longitudinal magnetoresistance of polycrystalline indium as a function of lattice resistivity.

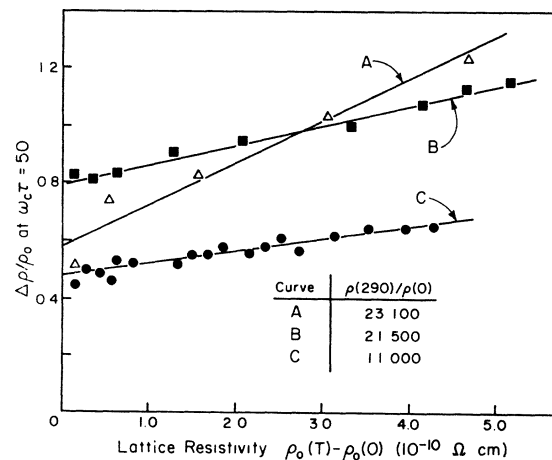


FIG. 7. Field dependence of the high-field Hall coefficient of two polycrystalline indium specimens. The top curve was derived from dc measurements, the bottom curve from helicon measurements.

surements. We have confirmed his measurements on potassium using the dc method, and in addition to indium have also observed a field-dependent decrease in the Hall coefficient of aluminum and sodium.²⁰ It is worth remarking that the alkali metals exhibit a substantially greater decrease than the other metals, as much as 12% at 140 kG.

IV. CONCLUSIONS

The present existing theories of high-field galvanomagnetic phenomena in metals make two specific predictions: (1) the longitudinal and transverse magnetoresistance of perfect metals with closed Fermi surfaces should saturate strictly in the high-field limit; and (2) the Hall coefficient in such metals should be independent of magnetic field, depending only on the relative concentrations of holes and electrons.

Our measurements on indium show these predictions to hold true in at best a semiquantitative sense or else only under certain restricted conditions. We have found the Hall coefficient of indium to be slightly field-dependent, even for $\omega_c\tau$ as high as 300, while the magnetoresistance is not only field-dependent at high fields, but shows dramatic departures from Kohler's rule. The shortcomings of the presently existing theories, however, do not appear to arise from an incorrect assessment of the influence of open orbits, magnetic breakdown, or band structure on charge transport. To the contrary, our studies show the Hall effect and magnetoresistance in indium to be so very nearly isotropic that it is difficult to attribute any of our anomalous findings to intrinsic features of crystal-structure or Fermi-surface topology. Rather the discrepancies between theory and experiment almost certainly result from an oversimplified or unrealistic treatment of the current relaxation mechanism. The common assumption of a simple isotropic relaxation time is likely to be valid in a real metal only for relatively impure samples—a situation in which the relaxation process is thoroughly dominated by large-angle impurity scattering. As could be expected, therefore, it is in our least-pure samples that we find the greatest agreement between theory and experiment; in fact, in these specimens we find the longitudinal magnetoresistance to exhibit complete saturation, exactly as predicted by the traditional theory. While the transverse magnetoresistance shows a tendency toward saturation, we definitely observe a weak field dependence at high fields with $\Delta\rho/\rho_0$ increasing approximately as $H^{1/2}$ in our least-pure specimens.

Pippard²² has suggested that in aluminum small-angle scattering between the second-zone hole surface and the third-zone electron surface could lead to an $H^{1/2}$ rise in the high-field transverse magnetoresistance. This increase with field, which is a general conse-

quence of the diffusion of carriers between hole and electron orbits, should not persist indefinitely, however, and at sufficiently high fields saturation is expected to be complete. Although this argument could be presumed to apply to indium also, we do not know whether this is the mechanism responsible for the $H^{1/2}$ field dependence which we have observed; because the magnetoresistance of indium in this purity range shows very little temperature dependence it appears unlikely to us that small-angle scattering from other sources could have a very strong effect.

It is in our highest-purity indium that the most pronounced deviations from the conventional theories have occurred, particularly with regard to magnetoresistance measurements. Specifically, we have found two distinct anomalies common to both the transverse and longitudinal magnetoresistance. First, in the high-field limit the resistance is not constant, but increases linearly with magnetic field, the rate of increase determined by some as yet undetermined scattering mechanism. Although this field dependence is not the result of impurity scattering, it is evidently not simply the result of small-angle scattering either, because low-energy phonon collisions are observed to have no detectable influence. Secondly, the "saturation value" of the magnetoresistance, which we define to be that high-field component, independent of field, does depend on both lattice resistivity and sample preparation history. The degree of enhancement of the saturation value is not a simple function of sample impurity content, however, but as discussed previously appears to depend on the mutual interaction of a number of scattering mechanisms.

A discrepancy between theory and experiment has also been observed to a lesser extent in measurements of the Hall effect, and many of the previous remarks also seem pertinent here. The decrease of the high-field Hall coefficient with field does not appear to be the result of explicit Fermi-surface features inasmuch as (a) no anisotropy has been observed and (b) we have noticed the effect to be even more pronounced in the alkali metals. Although our evidence is less complete here than with our magnetoresistance measurements, it is probably reasonable to conclude that relaxation processes other than ordinary impurity scattering are involved.

Thus, we conclude that while the existing theory may perhaps account satisfactorily for the high-field galvanomagnetic properties of bulk metals, additional theoretical work is required on the influence of various scattering mechanisms in real metals—mechanisms which become predominant only in the absence of impurity scattering. These include small-angle electron-phonon interactions, electron-electron collisions, and scattering due to extended lattice defects such as strain fields and slippage planes. These mechanisms have the common feature that they cannot be incorporated theoretically

²² A. B. Pippard, *Solid State Physics* (Gordon and Breach, Science Publishers, Inc., New York, 1969).

into a simple relaxation-time approximation, yet their effect on transport phenomena in high-purity metals may be profound. In fact, from an experimental point of view, measurements of the high-field magnetoresistance in high-purity metals may provide the most sensitive measure possible of the details of some of these subtle processes. In this regard, data on the longitudinal magnetoresistance of metals will probably be the most helpful because of the fact that the measured quantity ρ_{zz} is the simple inverse of σ_{zz} .

However, precise quantitative data on these sophisticated scattering mechanisms will probably be rather difficult to obtain. While it is relatively easy to regulate the temperature or impurity content of a metal, it is much more difficult to control, for example, the strain content or dislocation density. This difficulty is especially compounded by the fact that it is necessary, for the kind of measurements which we have described, to work with metals whose impurity content is so low that the residual resistivity is not dominated entirely by impurity scattering.

ACKNOWLEDGMENTS

The work above 100 Kg was performed at the National Magnet Laboratory at M.I.T. We wish to acknowledge the help given by the staff of that laboratory. We also wish to thank H. Taub and D. K. Wagner for contributions to this work.

APPENDIX: HELICON PROPAGATION IN TRANSVERSE CYLINDER

We are considering solutions to the helicon equation for a cylindrical sample of finite length whose major axis is transverse to a large static magnetic field \mathbf{B}_0 . This geometry is shown in Fig. 8 with the appropriate coordinate system. For a simple metal with conductivity σ and Hall coefficient R we have the constitutive relation, in rationalized MKS units,

$$\mathbf{E} + R\mathbf{j} \times \mathbf{B} = (1/\sigma)\mathbf{j}. \quad (\text{A1})$$

We write $\mathbf{B} = \mathbf{B}_0 + \mathbf{b}(\mathbf{r}, t)$ where \mathbf{B}_0 is the static uniform

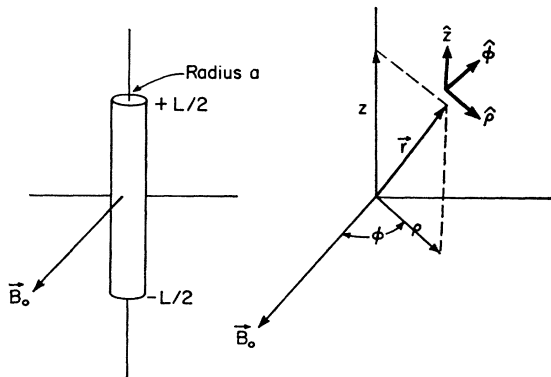


FIG. 8. Transverse cylinder geometry and coordinate system.

magnetic field, and it is assumed that $|\mathbf{b}| \ll |\mathbf{B}_0|$. Taking the curl of (A1) and making use of Maxwell's equations, we obtain the well-known helicon equation

$$\mu_0 \partial \mathbf{b} / \partial t = R \nabla \times [(\nabla \times \mathbf{b}) \times \mathbf{B}_0] + (1/\sigma) \nabla \times (\nabla \times \mathbf{b}) = 0. \quad (\text{A2})$$

We will suppose for the present that $1/\sigma = 0$ and neglect the third term in Eq. (A2); although the inclusion of this term is straightforward, the calculations become needlessly complicated. We will state the results of including a finite sample conductivity in our calculations, however.

In cylindrical polar coordinates, the three components of Eq. (A2) become

$$\partial b_\rho / \partial t - (RB_0/\mu_0) \nabla^2 b_z \sin \phi = 0, \quad (\text{A3a})$$

$$\partial b_\phi / \partial t - (RB_0/\mu_0) \nabla^2 b_z \cos \phi = 0, \quad (\text{A3b})$$

$$\begin{aligned} \partial b_z / \partial t + (RB_0/\mu_0) [\nabla^2 b_\rho - b_\rho/\rho^2 - (2/\rho^2)(\partial b_\phi / \partial \phi)] \\ \times \sin \phi + (RB_0/\mu_0) [\nabla^2 b_\phi - b_\phi/\rho^2 \\ + (2/\rho^2) \partial b_\rho / \partial \phi] \cos \phi = 0, \end{aligned} \quad (\text{A3c})$$

where we have written $\mathbf{b} = (b_\rho, b_\phi, b_z)$ and where

$$\nabla^2 b_i = -\frac{1}{\rho} \frac{\partial}{\partial \rho} \left(\rho \frac{\partial b_i}{\partial \rho} \right) + \frac{1}{\rho^2} \frac{\partial^2 b_i}{\partial \phi^2} + \frac{\partial^2 b_i}{\partial z^2}.$$

There are three solutions to these three coupled equations. Two of them relate b_ρ and b_ϕ to b_z and are given by

$$b_\rho = -ib_z \sin \phi, \quad (\text{A4})$$

$$b_\phi = -ib_z \cos \phi. \quad (\text{A5})$$

Making use of (A4) and (A5) then reduces each of the components of (A3) into the equation for b_z

$$+i \partial b_z / \partial t + (RB_0/\mu_0) \nabla^2 b_z = 0. \quad (\text{A6})$$

Equation (A6) may be readily solved by standard techniques to yield the general solution for b_z

$$b_z(\rho, \phi, z, t) = b_0 e^{+i\omega t} e^{\pm ikz} e^{\pm in\phi} J_{\pm n}(k'\rho). \quad (\text{A7})$$

Here $J_n(k'\rho)$ is the Bessel function of the first kind of integral order n , and ψ , k , and k' are related according to

$$\omega = -(RB_0/\mu_0)(k'^2 + k^2). \quad (\text{A8})$$

If we now incorporate into these solutions the effect of a finite sample conductivity σ , the only consequence is to slightly modify Eq. (A8) to include a damping term:

$$\omega = -(RB_0/\mu_0)(k'^2 + k^2)(1 + i/u), \quad (\text{A8}')$$

where $u = RB_0\sigma$ is the tangent of the Hall angle.

Solutions (A4), (A5), and (A7) reproduce the features of the well-known helicon mode; the magnetic field vector $\mathbf{b}(\mathbf{r}, t)$ rotates in the plane perpendicular to the static magnetic field \mathbf{B}_0 with the same sense of polarization as the carrier cyclotron rotation. (A field rotation in the opposite sense leads to a nonpropagating

mode which corresponds to the ordinary skin effect.) We remark that up to this point we have made no approximations other than to neglect the displacement current in Maxwell's equations and to make the linearizing assumption that $|\mathbf{b}| \ll |\mathbf{B}_0|$.

We will now consider solutions to the boundary-value problem appropriate to the sample geometry shown in Fig. 8. Extensive discussions of the correct boundary conditions have been given by Legendy,²³ who concluded that the appropriate boundary condition was simply the continuity of all magnetic field components at the boundary. In his treatment the vacuum field was divided into a "driving" field which was set up by the driving currents alone, and a "reflected" field due to the currents in the sample. Our treatment is a less sophisticated one which neglects the reflected field; it is, in this respect, more in line with the analysis of Chambers and Jones,¹⁵ in which the helicon field inside the metal was simply assumed to match the driving field at the sample boundary. While neglect of the reflected field leads to a 5% error in the expected frequency of the helicon for finite rectangular plates, we might expect the error inherent in this approximation to be substantially greater for cylindrical samples in which it is possible to approximate only one infinite dimension. While we have indeed found this to be the case, our simple treatment nevertheless reproduces the qualitative features of the observed standing-wave resonances in cylindrical specimens.

We suppose that the driving field $\mathbf{b}_0(t)$ is spatially invariant and directed along the $\phi = \frac{1}{2}\pi$ direction. The axis of the pickup coil is oriented at right angles to both the driving field and \mathbf{B}_0 and thus detects the mean field \bar{b}_z averaged over the entire sample. From Eq. (A7) it can be seen that only the $n=0$ components of b_z will result in a nonzero net flux, so that it is necessary only to evaluate an expression of the form

$$\bar{b}_z \propto \int_0^{k'a} (k'\rho) J_0(k'\rho) d(k'\rho) \int_{-kL/2}^{+kL/2} e^{ikz} d(kz) \\ = (k'a) J_1(k'a) \sin(\frac{1}{2}kL). \quad (\text{A9})$$

Making use of elementary Bessel-function identities we immediately conclude that the maxima in b_z will occur for

$$k'a = S_{0n} \\ \frac{1}{2}kL = (2m+1)\frac{1}{2}\pi \quad m = 0, 1, 2, \dots, \quad (\text{A10})$$

where S_{0n} is the n th zero of the zero-order Bessel function $J_0(x)$. Therefore, the dispersion relation for the standing-wave helicon resonance in a transverse

²³ C. R. Legendy, Phys. Rev. 135, A1713 (1964).

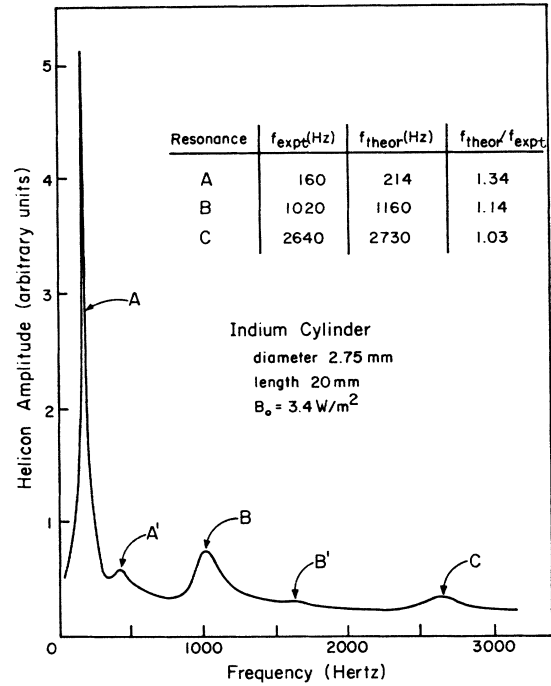


FIG. 9. Standing-wave helicon resonances in polycrystalline indium cylinder. Unprimed letters refer to primary resonances, while primed letters denote minor modes.

cylinder according to this simplified treatment is given by:

$$\omega_{nm} = -\frac{RB_0}{\mu_0} \left(1 + \frac{1}{n^2}\right)^{\frac{1}{2}} \left[\frac{S_{0n}^2}{a^2} + \frac{(2m+1)^2\pi^2}{L^2} \right]. \quad (\text{A11})$$

The primary resonances will occur at frequencies ω_{n0} and each will be accompanied by numerous "satellite" resonances occurring at ω_{nm} ; these are exactly analogous to the minor modes observed by Merrill, Taylor, and Goodman²⁴ in rectangular plates of sodium.

Figure 9 shows the standing-wave helicon resonances obtained for a thin polycrystalline indium cylinder. The primary resonances are identified by the unprimed letters, while the primed letters are thought to denote minor modes or satellite resonances. Figure 9 also shows the agreement between measured resonant frequencies and the frequencies predicted by Eq. (A11). Although the theoretical frequency is in error by 34% for the fundamental mode, the agreement becomes substantially better for the higher-order modes; for the $n=3$ resonance the discrepancy is only 3%, which lies well within the experimental error.

²⁴ J. R. Merrill, M. T. Taylor, and J. M. Goodman, Phys. Rev. 131, 2499 (1963).